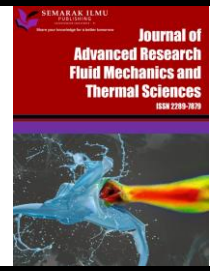




Journal of Advanced Research in Fluid Mechanics and Thermal Sciences

Journal homepage:
https://semarakilmu.com.my/journals/index.php/fluid_mechanics_thermal_sciences/index
ISSN: 2289-7879



Experimental Analysis of Various Implementations Quantity of Hollow Circular Fins on Solar Still Seawater Desalination

Muhamad Dwi Septiyanto^{1,3}, Firmansyah Alwi Sasongko¹, Syamsul Hadi^{1*}, Eko Prasetya Budiana¹, Irfan Santosa^{3,4}, Catur Harsito²

¹ Department of Mechanical Engineering, Faculty of Engineering, Universitas Sebelas Maret, Surakarta, Indonesia

² Mechanical Engineering, Faculty of Vocational School, Universitas Sebelas Maret, Surakarta, Indonesia

³ Mechanical Engineering, Faculty of Engineering, Universitas Sebelas Maret, Surakarta, Indonesia

⁴ Department of Mechanical Engineering, Faculty of Engineering, Universitas Pancasakti Tegal, Indonesia

ARTICLE INFO

Article history:

Received 9 December 2023

Received in revised form 26 April 2024

Accepted 14 May 2024

Available online 30 May 2024

Keywords:

HCF; solar still; efficiency; productivity

ABSTRACT

This present study conducted an experimental analysis of the use of hollow circular fins (HCF) within the conventional single-slope solar still (CS4) chamber. To enhance energy absorption, the optimal HCF numbers were increased by the available chamber space. The three identical CS4 testing chambers were examined in the climatic conditions of the Sebelas Maret University Faculty of Engineering, located in Ketingan, Surakarta, Indonesia. The HCF absorber is implemented with 176 HCF, 176 HCF, and 216 HCF within the chamber space. The findings indicate that there is a direct correlation between the increased HCF numbers and both productivity and efficiency. The efficiency for 117 HCF, 176 HCF, and 216 HCF is 27.04%, 35.20%, and 42.16% respectively. Therefore, it was determined that correlation analysis significantly contributed to the relationship between the HCF implementation and the different radiation intensities in day-to-day testing. To obtain a more comprehensive analysis, the randomized complete block design (RCBD) experiment in collaboration using least squares regression was conducted to compare the experimental production of CS4 with its predicted value.

1. Introduction

The earth consists of 75% water, but the majority of it is saltwater, which is not suitable for human consumption and fulfills the needs of human life [1]. The United Nations Organization predicts that clean water shortages, especially in coastal areas, will affect as many as 1800 million people by 2025 [2]. Therefore, purifying seawater with desalination devices can effectively fulfill the demand for clean water [3]. Desalination is the common term for the process of purifying saltwater into clean water for consumption [4]. Additionally, it is used to treat a variety of water types, including seawater, brackish, and river water. Naturally, seawater desalination accounts for approximately 67%, brackish water for 19%, river water for 8%, and wastewater for 6% of the total application of

* Corresponding author.

E-mail address: syamsulhadi@ft.uns.ac.id

<https://doi.org/10.37934/arfmts.117.2.172191>

desalination systems worldwide. The dominant countries that use the desalination process to produce clean drinking water are Saudi Arabia, Kuwait, the UAE, Qatar, Oman, and Bahrain [5].

A single-slope solar still (CS4) is a type of solar still that operates as an indirect passive system for purifying seawater into freshwater [3]. Generally, this type of solar still is an eco-friendly technology that relies on solar energy as its primary source [5,6]. The process of evaporating seawater involves the movement of saturated vapor within the chamber space through natural convection (Figure 1). This vapor then condenses into film droplets on partition glass on a particular slope. Recently, CS4 has emerged as a simple desalination technology that is user-friendly and has low construction expenses [7,8]. For instance, Elsheikh *et al.*, [8] conducted a study on the operational use of bilayered structures in solar stills. They estimated the construction expenses to be 0.15 dollars per liter of fresh water; however, the study found that CS4 desalination devices are generally more economically efficient for ensuring a sustainable future [8]. In the last decade, there has been extensive investigation into different aspects of desalination research and development. These include utilizing absorber plates to enhance heat absorption, employing phase change materials for latent heat storage, utilizing nanoparticles to improve thermal performance, and integrating phase change material with fin absorbers [9-17].

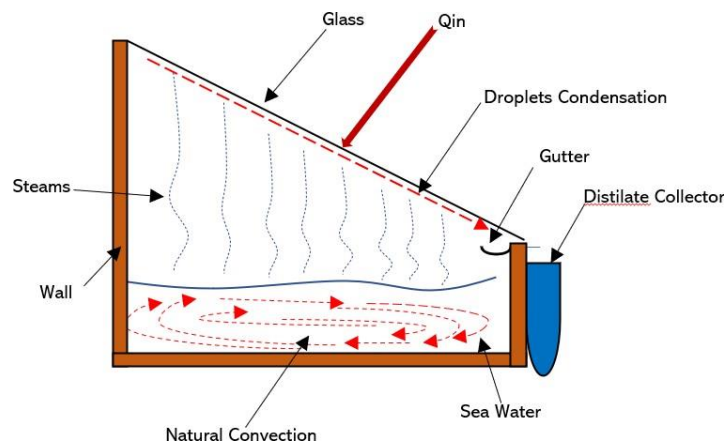


Fig. 1. Single slope solar still desalination

Several scholars have examined research on the use of absorber fins in desalination systems. El-Sebaai *et al.*, [18] employed several effects of fin absorber configurations. According to this study, productivity declines from 5,377 kg/m² to 4,802 kg/m² as the number of fins increases. This is because the additional fins cast shadows on adjacent fin areas, limiting the probability of heat absorption [18]. Furthermore, Elgendi *et al.*, [19] conducted a study utilizing variations of the Distributed Heat Sink (DHS) 49-block heat sink and the Group Heat Sink (GHS). The results for DHS and GHS exhibit a 24%-30% increase compared to the conventional single-slope type [19]. The article solely discusses the distribution of energy received by GHS, which was found to be more efficient compared to DHS. Nevertheless, it lacks to offer a comprehensive explanation of the physical phenomenon about the intensity of solar radiation the device absorbs and the energy losses it encounters [19]. Moreover, Miramoto *et al.*, [20] conducted research on the same concept, but with a greater number of horizontally-oriented fins. Three other types of experiments, specifically flat absorbers, flat 10 fins, and flat 15 fins, yielded daily water outputs of 1,185 L/day, 1,264 L/day, and 1,404 L/day, respectively [20]. The main objective of implementing the fin absorber in the CS4 desalination system is to assess the production efficacy, efficiency, and the amount of energy absorbed by the system. Fayaz *et al.*, [21] added that the utilization of a metallic titanium plate absorber could provide an appropriate surface temperature for the development of thermal operating solar stills. In regard to the various

applications of fin absorbers, Table 1 provides a comprehensive summary of the differences between solar stills and those with fin absorbers.

Table 1
 The related earlier study that utilized an absorber fin on desalination

Ref.	Case	Variations	Solar Still Type	Result
Abdelgaied <i>et al.</i> , [22]	Comparing the productivity of hollow circular and hollow square fins	Thickness of hollow circular and hollow square fins	Tubular solar still	Productivity: 6.11 liters (hollow circular fin) and 5.52 liters (hollow square fin)
Wang <i>et al.</i> , [23]	Comparing the performance of vertical and horizontal fin directions	Vertical and horizontal fins	Tubular receiver	The vertical fin has better heat transmission capabilities compared to the horizontal fin
Jani and Modi [24]	Comparing the performance between the circular and square fins	Hollow circular and square fins	Pyramid solar still	Circular fin productivity was 54.22% higher than square fin
Alaian <i>et al.</i> , [25]	Comparing the productivity between the conventional solar still and pin fin	Circular pin fin	Single-slope solar still	Improved efficiency by 23% compared to conventional
Appadurai and Velmurugan [26]	Comparing productivity between conventional and pin-type solar ponds	Fin-type solar pond	Single-slope solar still	50% productive increase over conventional solar still
Velmurugan <i>et al.</i> , [27]	Comparing the productivity between the conventional and rectangular pin	Solid rectangular fins	Single-slope solar still	Increased productivity by 75% more than conventional solar still

Extensive research has been conducted on the utilization of absorber heat in solar desalination systems, incorporating various modifications to the fins' shape. The literature employed different types of fins, including pin fins, circular fins, rectangular fins, hollow circular fins, and others [25,26,28-30]. Furthermore, several studies have investigated the utilization of fins in different solar still designs, including the Pin Fin type with FLBS solar still, a flat horizontal fin on single slope solar still, and a heat sink type fin on pyramid solar still [18-20]. Despite the variation in the number of fins in those articles, the information provided showed a large fin gap that might cause inefficiency in consuming the entered energy even though the fin was already in use. In addition, the analysis solely takes into account the fluctuation of solar radiation intensity as an element of uncertainty factor and does not incorporate a component for quantification effect on solar still production. Therefore, the conclusion of the research undermines the suitability of the results for concluding the broader study since the effective contribution between the main variation and nuisance (different radiation intensity day-to-day testing) is still unquantified. Hence, this experimental study aimed to enhance the efficiency of CS4 by incorporating an absorber fin and evaluating the effective contribution parameter of various radiations in day-to-day testing. The study was also conducted with a distinct fin type compared to earlier studies while considering the amount of HCF under the chamber space's maximum capacity. The first limitation of this study was that it did not account for the sudden shift in weather from sunny to cloudy because it's running fast. The heat loss calculation through conduction from saltwater to the wall and insulation was estimated using a linear equation, $Q_b + Q_w$. In the meantime, the final heat propagation of water to the internal air and then to the water glass was calculated and estimated by the $Q_{T,go-a}$.

2. Heat Loss Analysis

The energy obtained by the solar still is not completely absorbed for seawater evaporation. Figure 2 illustrates the boundary and energy distribution of the testing chamber, taking into account the heat loss.

2.1 Heat Loss of the Glass Outer Surface

The partition glass can lose heat to the surroundings through convection and radiation. Eq. (1) represents radiation heat loss on the glass surface.

$$Q_{R,go-a} = h_{R,go-a} \times (T_{go} - T_a) \quad (1)$$

The radiation coefficient ($h_{R,go-a}$) can be described as follows

$$h_{R,go-a} = \varepsilon_g \sigma \left[\frac{(T_{go}+273)^4 - (T_{sky}+273)^4}{T_{go} - T_a} \right] \quad (2)$$

The temperature of the sky can be defined as follows

$$T_{sky} = T_a - 6 \quad (3)$$

The convection heat loss that occurs on the partition glass is linked with the surroundings as component of the reflected energy within the system. The equation representing convection heat losses is as follows

$$Q_{c,go-a} = h_{c,go}(T_{go} - T_a) \quad (4)$$

Meanwhile, the convection heat transfer coefficient is determined using the equation given below

$$h_{c,go-a} = 2.8 + (3.0 \times v) \quad (5)$$

Therefore, the total heat loss of partition glass can be represented as follows

$$Q_{T,go-a} = Q_{c,go-a} + Q_{R,go-a} \quad (6)$$

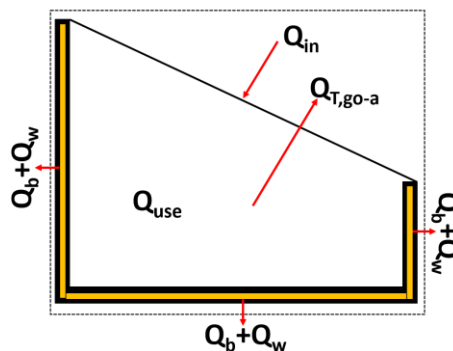


Fig. 2. Research boundary condition

2.2 Wall-side Heat Loss

The energy loss is additionally accounted for through the side and bottom walls of the solar still. The heat dissipated can be analyzed as heat transfer processes involving convection (Eq. (7)) and conduction (Eq. (8)) [31]. Where the value of the heat transfer coefficient h_b can be written as a function in Eq. (9).

$$Q_w = h_w(T_{ch} - T_w) \quad (7)$$

$$Q_b = h_b(T_{ch} - T_a) \quad (8)$$

$$h_b = \left[\frac{L_{insulation}}{K_{insulation}} + \frac{1}{h_{R,b-a}} \right]^{-1} \quad (9)$$

$$h_{R,b-a} = 5.6 + (3.8 \times v) \quad (10)$$

Thereby, Eq. (11) represents the coefficient of heat loss at the bottom of the wall. Meanwhile, the heat loss coefficient on the side wall is given by Eq. (12). Hence, the overall heat loss transfer coefficient for the side and bottom walls can be determined by employing Eq. (13).

$$U_b = \frac{h_w \times h_b}{h_w + h_b} \quad (11)$$

$$U_{sw} = \frac{A_{ss}}{A_b} \times U_b \quad (12)$$

$$U_{bs} = U_b + U_{ss} \quad (13)$$

2.3 Efficiency

The final effectiveness of desalination is determined by the solar efficiency, which is represented by Eq. (15). Efficiency, particularly in the context of desalination, was defined as the quotient of the total latent heat and productivity divided by the entering radiation intensity [12,31].

$$\eta_{passive} = \frac{\sum m_{ew} \times h_{fg}}{\sum I(t)_s \times A_s \times 3600} \quad (14)$$

When the input energy Q_{in} , τ represented transmissivity, $I(t)$ symbolized radiation intensity, and A denoted the cover area. Eq. (14) provides the input energy for S4. In addition, S4 utilized the energies to vaporize the seawater described in Eq. (15), where M_{ew} represents the mass of water condensation (Kg), M_{ch} was the seawater mass within the chamber (Kg) and h_{fg} was the enthalpy (kJ/kg) [20].

$$Q_{in} = \tau \times I(t) \times A \quad (15)$$

$$Q_{use} = \frac{M_{ew} \times h_{fg}}{t} + \frac{M_{ch} \times C_p \times \Delta T}{t} \quad (16)$$

$$h_{fg} = 1000 \times (2501.9 - 2.40706 T_w + 1.192217 \times 10^{-3} \times T_w^2 - 1.5863 \times 10^{-5} \times T_w^3) \quad (17)$$

3. Material and Method

3.1 Basin and Fin Configurations

The solar still had the following dimensions: a length of 1030 mm, a width of 765 mm, a front height of 8.6 mm, a back height of 402 mm, and a glass tilt of 25° (Figure 3). The single-slope passive solar still was positioned on a table at a height of 770 mm. The wall of S4 was constructed using plywood material with hardwood, heat resistance, and anti-curvature [32]. Additionally, the inner wall of the S4 chamber was coated with a stainless-steel substance absorber. This material was specifically designed to optimize the absorption of heat obtained from solar radiation. Furthermore, as an addition to the experiment, hollow circular fins with quantities of 117, 176, and 216 were employed as supplementary absorbers. The additional hollow circular fins used for research purposes had dimensions of 12.5 mm in diameter and 40 mm in height.

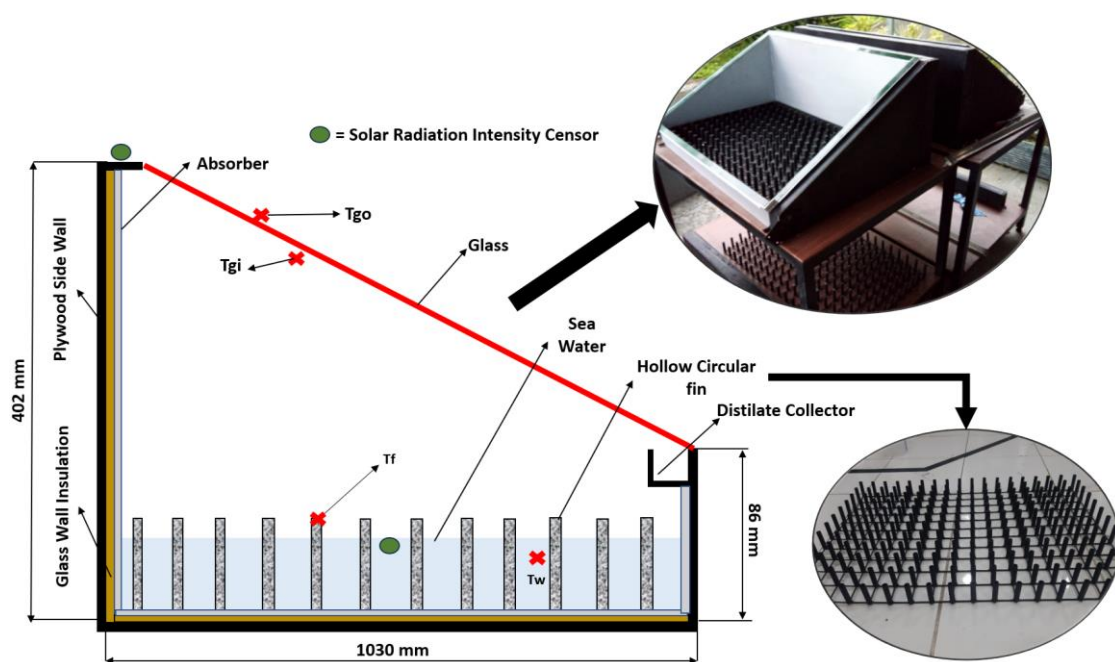


Fig. 3. Set-up CS4 testing chamber

3.2 Data Capturing

The data was collected using three S4 basins that had been previously calibrated or tested. The process was carried out once all three achieved identical levels of distilled water productivity. This research flowchart is illustrated in Figure 4. The investigation was carried out in Kentingan, Surakarta, throughout the summer climate for five consecutive days from July 27th to July 31st, 2022, from 7 a.m. to 6 p.m. (GMT +7). Thermocouples were utilized to measure the temperature, and they were connected to the data logger. The installation involves measuring the temperatures of various components, including the seawater temperature inside the basin (T_w), the temperature of the hollow circular fins (T_f), the temperature of the inner glass (T_{gi}), and the temperature of the outer glass (T_{go}). Figure 2 depicts all temperature measurement devices in their respective locations. The BTM-4208SD Data Logger documented the process of collecting temperature data, which included measurements of T_w , T_{ig} , T_f , and T_{og} . The data recording was set automatically at hourly intervals. Moreover, the intensity of the solar radiation data had a substantial impact on the efficiency of the S4 desalination process [24]. The radiation intensity received by the S4 basin was measured using an

SPM-1116SD solar power meter. The desalinated water that condenses on the inner surface of the glass is collected through the gutter and sent into the measuring cup. Subsequently, the productivity data, which includes the fluctuating total radiation received, is utilized for correlation analysis. This analysis calculates the predicted data analysis and measures the significant contribution factor between the HCF implementation and solar intensity fluctuations.

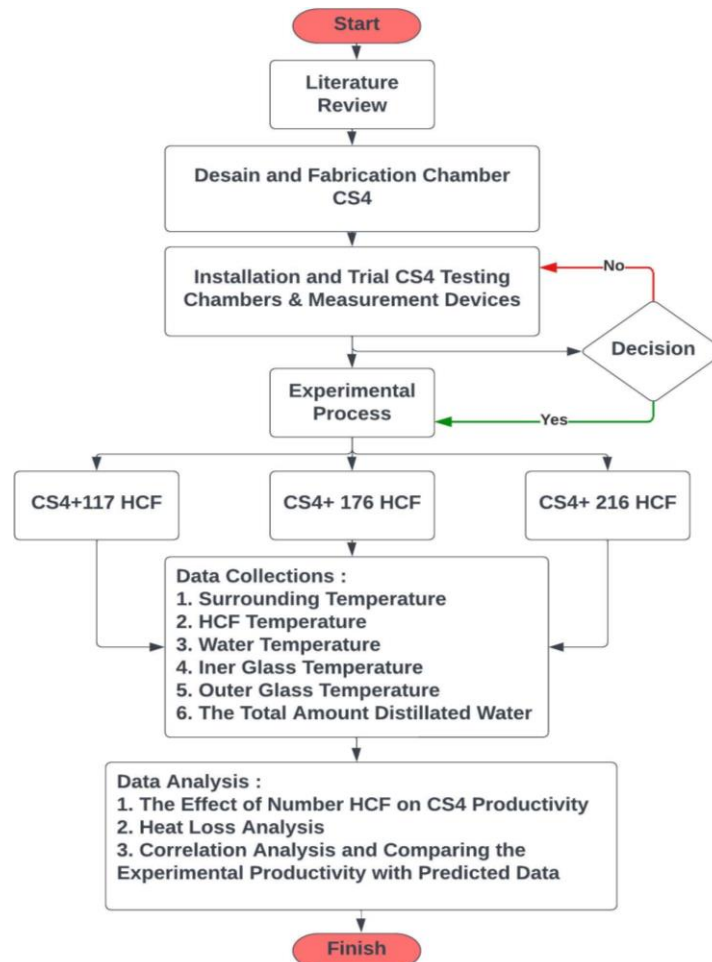


Fig. 4. Flowchart experiment

3.3 Uncertainty Analysis

The experiments utilized measurement instruments that incorporated both uncertainty and measurement ranges, as indicated in Table 2. An error analysis can quantify errors in temperature (∂T), radiation intensity (∂I_t), productivity (∂M_{ew}), latent heat (∂h_{fg}), and solar still efficiency ($\partial \eta$). This estimation is derived from the propagation error formulation, which takes into account both random error (∂R) and bias error (∂B) as described in Eq. (18). The biased error in this study is determined by the accuracy of the measurement devices, whereas the random error is influenced by the fluctuations of the data obtained from the measuring devices. A similar error analysis model was also presented in a correlated study by Nagaraju *et al.*, [33]. Here are several equations that represent the consideration of error.

Table 2
 Uncertainty and device specification

Measurement Devices	Accuracy	Range
Measurement Glass	±1 mL	0-2000 mL
Solar Power Meter	± 10 W/m ²	0-2000 W/m ²
K- type Thermocouple	± 0.1°C	0-650°C

$$\partial X = \sqrt{\partial R^2 + \partial B^2} \quad (18)$$

$$\Delta T = \sqrt{(\partial T_1)^2 + (\partial T_2)^2 + (\partial T_3)^2 + (\partial T_4)^2 + (\partial T_5)^2 \dots + (\partial T_n)^2} \quad (19)$$

$$\Delta M_{ew} = \sqrt{(\partial M_{ew1})^2 + (\partial M_{ew2})^2 + (\partial M_{ew3})^2 + (\partial M_{ew4})^2 + (\partial M_{ew5})^2 \dots + (\partial M_{ewn})^2} \quad (20)$$

$$\Delta I_t = \sqrt{(\partial I_{t1})^2 + (\partial I_{t2})^2 + (\partial I_{t3})^2 + (\partial I_{t4})^2 + (\partial I_{t5})^2 \dots + (\partial I_{tn})^2} \quad (21)$$

$$\Delta h_{fg} = \sqrt{\left(\frac{\partial h_{fg}}{\partial T_w} \times \Delta T_w\right)^2} \quad (22)$$

$$\partial \eta = \sqrt{\left(\frac{\partial \eta}{\partial M_{ew}} \times \Delta M_{ew}\right)^2 + \left(\frac{\partial \eta}{\partial h_{fg}} \times \Delta h_{fg}\right)^2 + \left(\frac{\partial \eta}{\partial I_t} \times \Delta I_t\right)^2 + \left(\frac{\partial \eta}{\partial A} \times \Delta A\right)^2} \quad (23)$$

The 6% estimated error is derived from the equation provided for this experimental analysis. The HCF fin implementation serves as the independent variable, whereas the performance of the CS4 chamber functions as the dependent variable. Fluctuations in the daily received radiation were a component that needed to be taken into account, as the productivity outcomes observed on the experimental days were influenced by different levels of incoming radiation. Therefore, the Randomized Block Complete Design (RCBD) study analysis grouping model is employed to categorize the level of solar radiation as a nuisance or Block factor. Consequently, a correlation analysis was performed to examine the relationship between the variable of HCF amount and solar intensity, and the dependent variable of CS4 productivity. In addition, the RCBD model allows the estimation of the correlation between the main factor (HCF) and the nuisance factor by comparing the experimental data with the study of CS4 production data using the Root Mean Square Error (RMSE).

$$RMSE = \sqrt{\frac{\sum_1^n ((M_{ew})_{exp} - (M_{ew})_{predic})^2}{n}} \quad (24)$$

$$Y = BX_1 + BX_2 + C \pm RMSE \quad (25)$$

$$SE(HCF) = \beta_{HCF} \times r_{cor} \times 100\% \quad (26)$$

$$SE(rad) = \beta_{rad} \times r_{cor} \times 100\% \quad (27)$$

4. Result and Discussion

This study primarily examined the solar radiation received by each testing chamber and explored the relationship between radiation intensity, hourly productivity, temperature, energy analysis, and correlation analysis.

4.1 Solar Radiation Intensity

The solar desalination process depended mainly on solar radiation intensity as it transformed into heat evaporation. The energy that passed through the partition glass was used for the process of seawater evaporation and was partially absorbed by HCF as sensible heat. Figure 5 depicts the increase in solar radiation intensity per hour over five days of testing. The total solar radiation entering the solar still system on each day, in consecutive order, was accumulated in 5885 W/m², 5794 W/m², 4882 W/m², 5761 W/m², and 5819 W/m². In consideration of the fluctuation in incoming solar radiation intensity, a single trendline was derived from the average solar radiation intensity received by the chamber (represented by the red lines) for the incoming energy analysis. Thus, the average accumulated solar radiation obtained was 5628 W/m². This is in line with the literature that solar intensity was a significant factor affecting the productivity and temperature efficiency of solar still performance [29]. Additionally, other literature suggests that wind speed and glass transmissivity were experimental productivity factors that might be disregarded [34,35]. Moreover, another piece of literature discussed the wind speed effect [36]. The experimental measurement of solar intensity yielded a R_{square} value of 0.915, as determined by the least squares correlation. This indicates that the data distribution of the radiation intensity received during the experiment is highly correlated and can be utilized to compare input energy calculations.

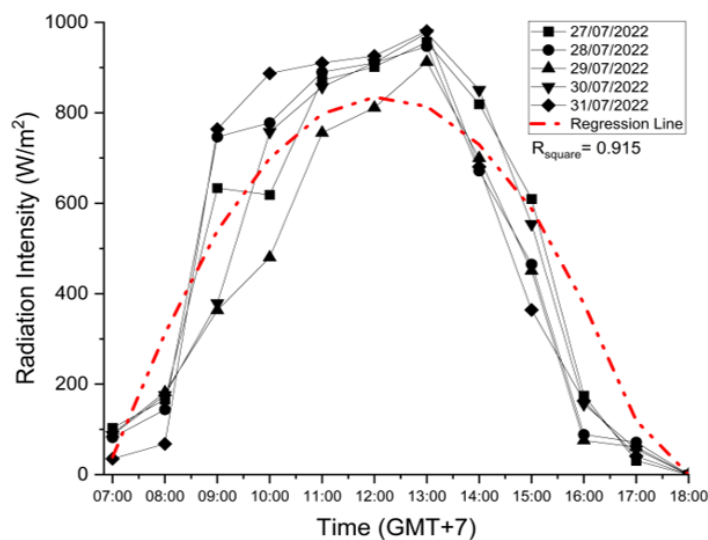


Fig. 5. The received radiation intensity during the daytime experiment

4.2 Relation Between Radiation Intensity, Temperature, and Hourly Productivity

Figure 6, Figure 7, and Figure 8 show the correlation between the average hourly production, the plotted internal temperature, and the received radiation intensity in each testing chamber with varying HCF numbers. According to that data, the average hourly production showed a direct relationship with both the radiation intensity and the internal temperature. The daily correlation of

received radiation, as measured by the R_{square} coefficient, remains consistently high at 0.915. This correlation was further improved by utilizing the RCBD model in this experiment, which assumes that the amount of energy entering remains constant throughout the day. Nevertheless, every testing chamber retains a distinct temperature. As an illustration, the highest recorded temperatures (T_f) for the HCF were 66.24°C, 69.44°C, and 71.30°C, respectively, at 117 HCF, 176 HCF, and 216 HCF. The HCF effect was observed on the final recorded seawater temperatures, specifically 37.48°C, 38.62°C, and 40.08°C. According to the research, the climate was found to be variable and unpredictable, as seen in both cloudy and sunny conditions. Sachan *et al.*, [37] explained that the implementation of this fin absorber offers advantages in mitigating the significant temperature drops that occur during unexpected changes in circumstances. Based on the preceding discussion, this result also shows that when the highest level of HCF is used, it can keep the temperature of the chamber space stable [37].

Jahanpanah *et al.*, [12] revealed that the desalination device's production rate is optimally achieved when there is a significant temperature difference in the basin. This experimental analysis showed a clear correlation between the research findings and Figure 6, Figure 7, and Figure 8. It was seen that there was a significant increase in average hourly productivity. Specifically, Figure 8 demonstrated that a temperature difference of 17.32°C resulted in the production of 94 mL.

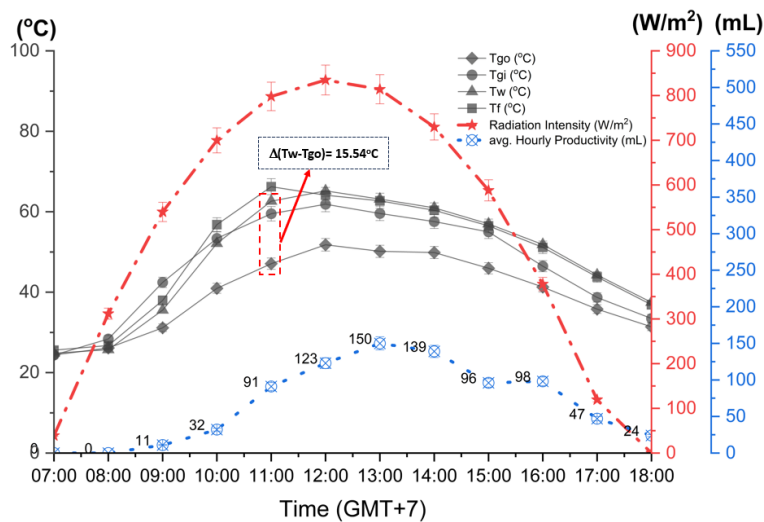


Fig. 6. The relationship between radiation intensity, temperature, and average hourly productivity at CS4 with 117 HCF

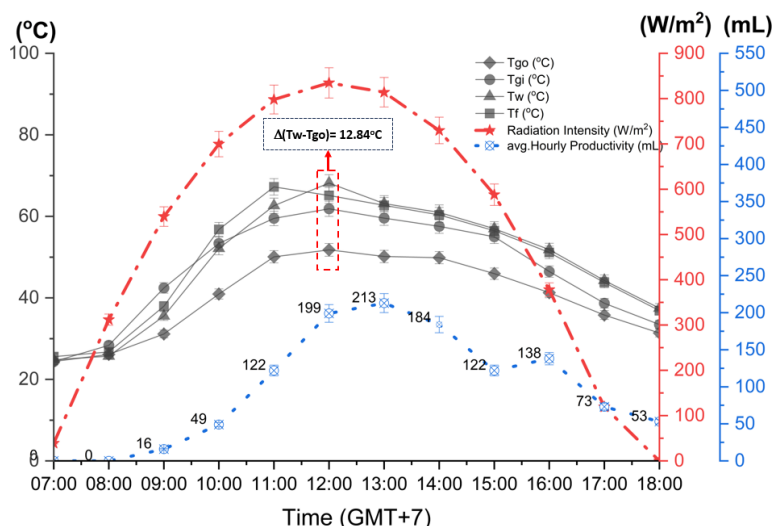


Fig. 7. The relationship between radiation intensity, temperature, and average hourly productivity at CS4 with 176 HCF

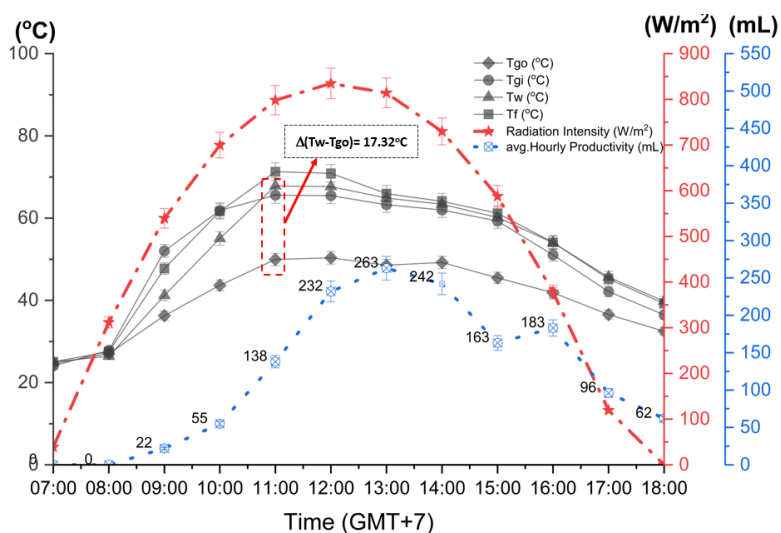


Fig. 8. The relationship between radiation intensity, temperature, and average hourly productivity at CS4 with 216 HCF

4.3 Efficiency

The study focuses on using the chamber's equilibrium efficiency and total productivity as the primary indicators to assess the effectiveness of the additional fin work. Figure 9(a) and Figure 9(b) illustrate the efficiency and total production of each variant during the performance testing. Eq. (14) determines the solar still's efficiency in this experimental analysis. According to Figure 9(b), the chamber with 216 fins had the highest total production of 1456 mL. This was followed by the chambers with 176 and 117 fins, which produced 1153 mL and 800 mL, respectively. The observed increase in productivity suggests that the 216 HCF may have stored the greatest amount of sensible heat from radiation intensity. This relationship is linear and is influenced by the size of the absorption surface [31,37]. This aligns with previous research that corroborated the observed trendline phenomenon in this study [38]. Meanwhile, the contrast between the present experimental analysis and the previous study is displayed in Table 3.

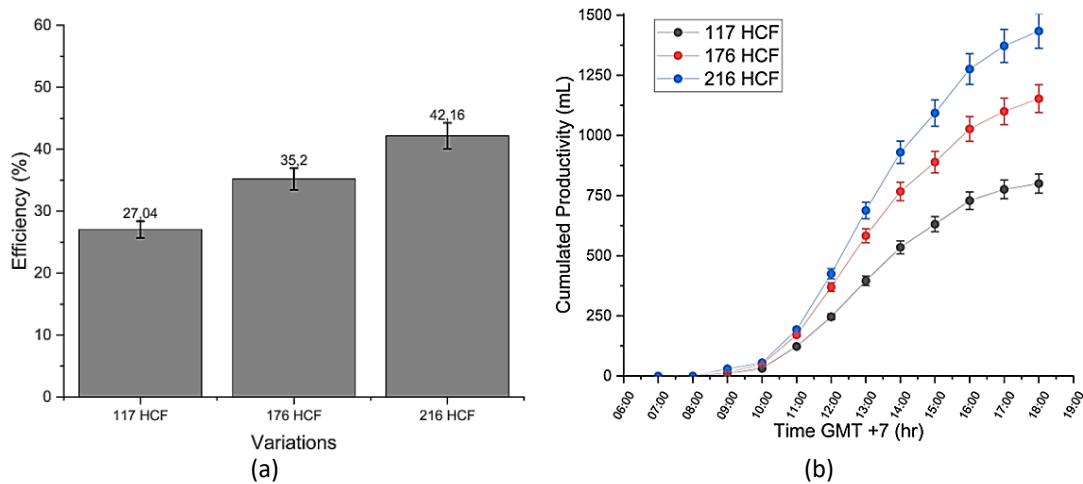


Fig. 9. The total (a) efficiency and (b) productivity of CS4

Table 3

Research comparisons

No.	Ref.	El-Sebaili <i>et al.</i> , [18]	Elgendi <i>et al.</i> , [19]	Mirmanto <i>et al.</i> , [20]	Present Study
1	The type of solar still	FLBS Solar Still	Pyramid Solar Still	Single Slope	Single Slope
2	Fin Type	Pin Fin	Heat Sink	Horizontal flat fin	Hollow Circular Fin
3	Month Operation	July - August	January - March	June	June
4	Chamber Area	1 m ² (absorber area)	Not given	1 m × 0.8 m × 0.571 m	1.03 m × 0.76 m × 0.402 m
5	Production	5.065 kg/m ² (n = 7) and 4.802 kg/m ² (n = 14)	3.434 kg/m ² (conventional), 3.302 kg/m ² (49 Blocks), and 3263 kg/m ² (1 Block)	1.185 kg/m ² (n = 15), 1.264 kg/m ² (n = 10)	1.456 kg/m ² (n = 216), 1.153 kg/m ² (n = 176), dan 0.8 kg/m ² (n = 117)
6	Efficiency	47.05% (n = 7) and 50.49% (n = 14)	31% (conventional), 34% (49 Blocks), and 33% (1 Block)	Between 24-33%	42.15% (n = 216), 35.20% (n = 176), and 27.04% (n = 117).

4.4 Energy Analysis

Figure 10 displays the productivity of each testing chamber in relation to the charging and discharging zones. The charging zone is the area where the HCF absorbs the inputted energy, while the discharging zone is where the absorbed heat is released to sustain the evaporation of seawater.

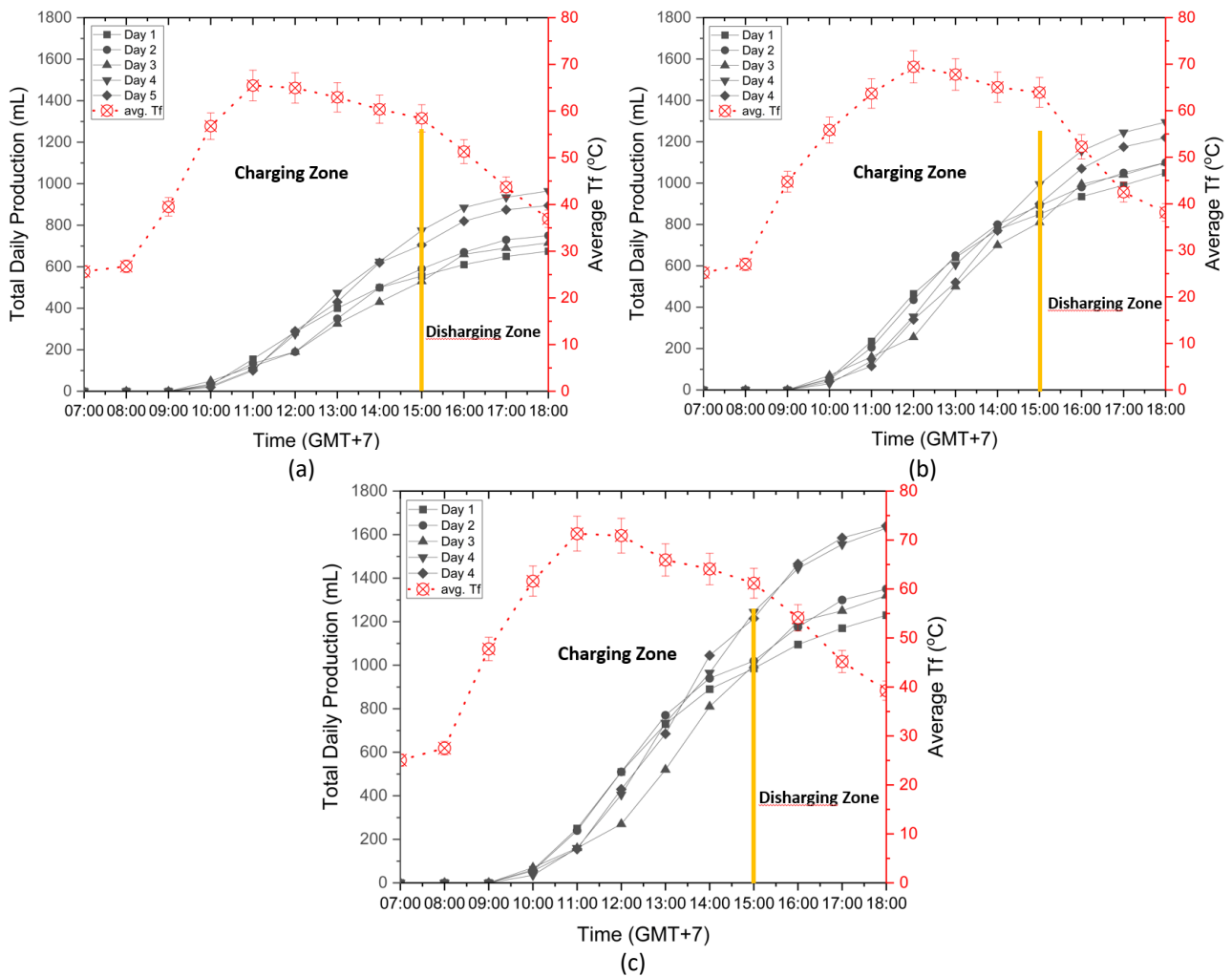


Fig. 10. Total daily productivity with the charging and discharging zone

From 7 a.m. to 8 a.m. (GMT +7), the incoming heat was utilized to increase the temperature of the seawater. However, only a portion of the heat was absorbed by the HCF, and it was insufficient to initiate the evaporation process. After 8 a.m., the heat that was required to evaporate and condense the film droplet into the internal chamber was introduced. At an energy level of zero (6 p.m.), each testing chamber carried out its desalination process. This resulted in productivity of 20 mL, 45 mL, and 55 mL for the chambers with 117 HCF, 176 HCF, and 216 HCF, respectively. The incorporation of HCF released 32.59 J, 55.77 J, and 67.45 J.

The amount of solar energy that is transferred into the internal chamber is greatly influenced by the transmissivity of the partition glass. This phenomenon is attributed to droplet film condensation, the thickness of the glass, and the type of material used [35,39]. Moreover, radiation is theoretically reflected in three distinct sections, including the partition glass, the seawater in the chamber, and the absorber plate [40]. However, this study employed a simple test that measured the discrepancy in radiation intensity reception error between the outside and inside sensors of the system. Consequently, the introduction of radiation was deemed to have a 2.2% margin of error due to the impact of tiny droplets. Subsequently, the quantity of Q_{in} was calculated using Eq. (15). Simultaneously, Q_{use} denoted the total energy consumed by S4, which was calculated using Eq. (16). According to Figure 11, the energy absorbed during the experiment remained quite low. However, efficient utilization of basin space was achieved by maximizing the number of hollow circular configurations. The HCF adequately absorbs the entered radiation intensity, thereby preventing a

considerable decrease in internal temperature during cloudy conditions. Between 3 p.m. and 4 p.m., there was an abnormal trendline observed in each testing chamber, accompanied by an increase in HCF. An abnormality can be characterized by the occurrence of a drop in temperature during a certain natural phenomenon. However, this drop is mitigated by the continuous release of energy from HCF, allowing for an increase in Q_{use} at 4 p.m. As a result, the chamber is currently undergoing the desalination process using a combination of energy from the limited radiation intensity and absorbed energy from HCF in the discharge zone. The dissipated energy from the system to the environment through the partition glass ($Q_{T,go-1}$) can be evaluated in terms of radiation using Eq. (1) and convention using Eq. (4). The total magnitudes and percentages were 1291.77 W (42.49%), 1174.50 W (38.65%), and 1505.43 W (49.52%) at 117 HCF, 176 HCF, and 216 HCF, respectively. Meanwhile, the total magnitudes and percentages of energy wasted through the top and bottom walls $Q_b + Q_w$ were 925.55 W (30.45%), 749.99 W (26.15%), and 252.47 W (8.30%) at 117 HCF, 176 HCF, and 216 HCF. It was discovered that reducing the gap between the fins in order to increase the evaporation area of the chamber can effectively reduce the amount of energy lost through the glass partition and the walls at the bottom of the chamber.

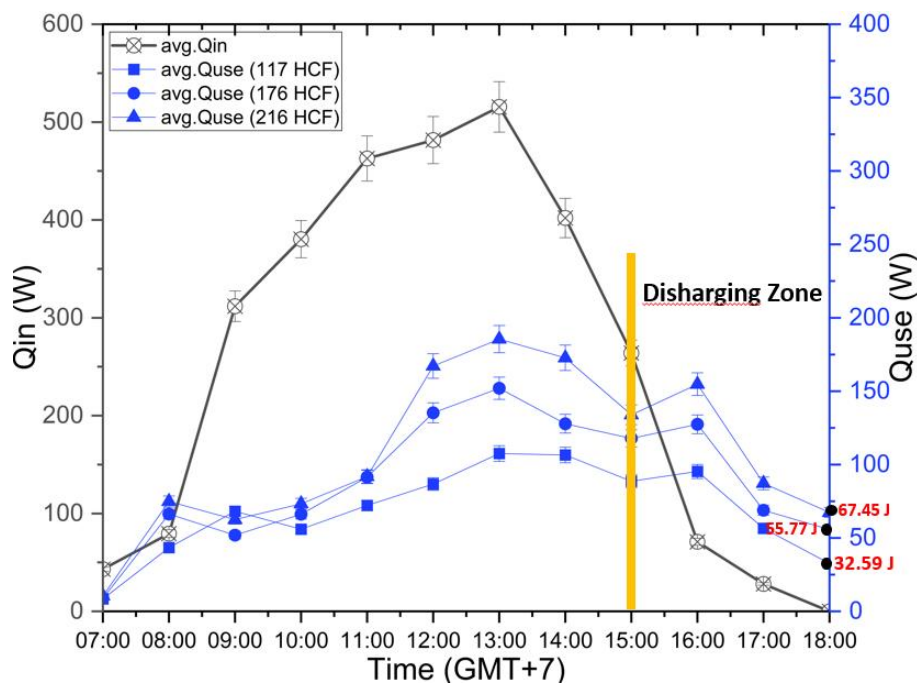


Fig. 11. The graph of Q_{in} and Q_{use} from each testing chamber

4.5 Correlation Analysis

The RCBD model, as proposed by Montgomery [41], was used to analyze the link between the effect of HCF usage and the influence of nuisance radiation intensity. The RCBD model refers to the single-factor analysis performed by the HCF implementation effect in this experiment. However, there were consequences of different amounts of day-to-day solar intensity that could not be disregarded; hence, it was employed as a nuisance factor or Block. The independent variables (main factor) in this study are 117, 176, and 216 HCF, while the different total radiation received by the testing chamber CS4 on the day of the experiment is represented as Block, which consists of Block 1 (5885 W/m²), Block 2 (5794 W/m²), Block 3 (4882 W/m²), Block 4 (5761 W/m²), and Block 5 (5819 W/m²) (Table 4). The statistical significance and correlation between the variables were tested using

ANOVA and linear least squares regression, respectively. It was inferred from the statistics that the significance threshold (α) equals 5%.

Table 4
 The grouping of productivity data using the RCBD model

Variation Number HCF	Block				
	1 (mL)	2 (mL)	3 (mL)	4 (mL)	5 (mL)
117 HCF	675	750	715	965	895
176 HCF	1050	1100	1100	1295	1220
2116 HCF	1230	1350	1320	1630	1640

Decision:

$H_0 = \text{Sig}_{\text{count}} > \alpha$ (The amount of HCF didn't have a significant effect on solar still productivity)

$H_1 = \text{Sig}_{\text{count}} < \alpha$ (The amount of HCF have a significant effect on solar still productivity)

The ANOVA statistical test in Table 5 presents the results that identify the parameters with the greatest influence on CS4 productivity. The experimental results unequivocally demonstrate that the productivity of CS4 exhibits a linear rise when HCF is introduced into the chamber. Additionally, as variations in the intensity of solar radiation received also play a significant role as a determining factor. Therefore, according to Table 5, the significance value (0.016×10^{-5}) for HCF was considerably smaller than α , indicating a strong relationship. Similarly, the significance value (22.824×10^{-5}) for radiation intensity likewise yielded the same conclusion. The HCF variation was found to be significantly smaller than α in comparison to the radiation intensity. This suggests that HCF variation plays a substantial role in enhancing the productivity of the CS4 chamber. Table 6 displays the results of the least squares linear regression test (Eq. (28)). The test was conducted to derive the equation for an optimum productivity prediction model of CS4, taking into account the influence of HCF numbers and radiation intensity as nuisance factors. Eq. (28) was derived from Eq. (25) to forecast the productivity of solar still. The accuracy of the model was evaluated using the RMSE of ± 272.97 . The study's R_{square} value was 0.970, showing a strong and statistically significant correlation between the independent and dependent variables. An outside factor, calculated to be 0.045, was found, presumably indicating a factor that is not influenced by the unpredictable changes in weather conditions between sunny and cloudy. By utilizing Eq. (26) and Eq. (27), the effective contribution of HCF and radiation intensity factor to CS4 productivity can be estimated at 80.10% and 13.91%, respectively.

Table 5
 The Anova testing result

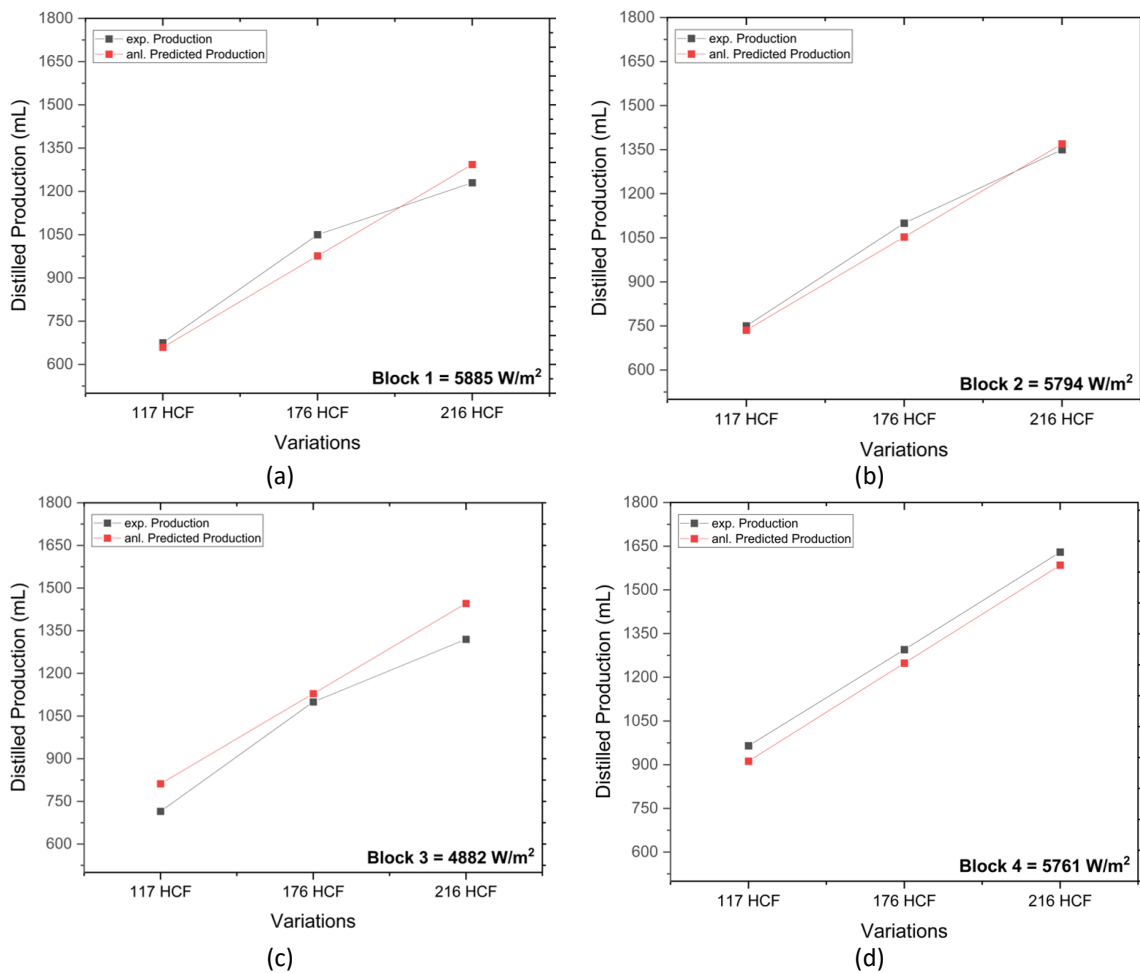
Dependent Variable: Productivity					
Source	Sum Square Error	df	Mean Square	F	Sig.
Corrected Model	19119615	6	19119615	340.646	5.071×10^{-5}
Variations (Number HCF)	1009210	2	504605	197.015	0.016×10^{-5}
Radiation (Block)	224510	4	56127.500	21.914	22.824×10^{-5}

Table 6
 The linear least squares regression method

Model	Unstandardized Coefficient		Standardized Coefficient (β)	Correlation Coefficient (r_{cor})	R_{square}
	B	Std. error			
(Constant)	266.000	68.998			0.970
Radiation (X_1)	76.333	14.387	0.373	0.373	
Variation HCF (X_2)	317.000	24.919	0.895	0.895	

$$Y = 76.333X_1 + 317X_2 + 266 \pm 272.97 \tag{28}$$

The productivity of CS4 can be graphically represented using the Eq. (28) model and subsequently compared to the empirical estimates of productivity. Meanwhile, Figure 12 shows the graph illustrating the experimental productivity in comparison to the analytically predicted production. The gap plotted between experiments and predictions occurs due to the error factor of experimental data collection and the limitations of measuring instruments.



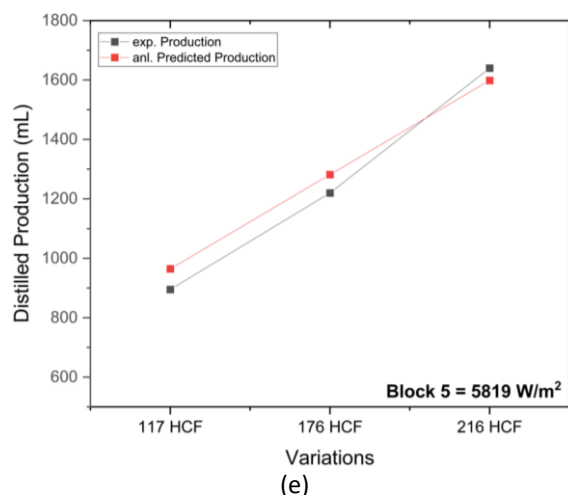


Fig. 12. The comparison of experimental and analytic production on (a) Day 1, (b) Day 2, (c) Day 3, (d) Day 4, and (e) Day 5

5. Conclusions

The experimental investigation of the additional hollow circular fins within the CS4 chamber has been successfully completed. The analysis section has explored the impact of the growing number of HCF on several factors such as productivity, internal temperature, energy analysis, and correlation analysis. Based on the experiments, numerous conclusions can be drawn, including

- i. The CS4 productivity reached its peak at 1456 mL when the maximum number of fins in basin was added to basin room 216. In contrast, the productivity was 1153 mL and 800 mL at 117 HCF and 176 HCF, respectively. Therefore, the additional absorbers exhibited a direct relationship with the solar still's production.
- ii. The radiation intensity factor was an important factor to be considered. This study found that radiation intensity accounted for a 13.91% contribution to the effect on solar still production.
- iii. The efficiency of chamber CS4 was 27.04%, 35.20%, and 42.16% for 117 HCF, 176 HCF, and 216 HCF, respectively.
- iv. The rate at which CS4 condensed on the partition glass was affected by the temperature difference between the outside temperature chamber and the inside glass. In particular, the chamber with an additional 216 HCF had a temperature difference of 17.32°C (at midday) and an average hourly condensation rate of 94 mL/hour.
- v. The energy losses through the partition glass to the surroundings were 42.49%, 38.64%, and 49.52% at 117 HCF, 176 HCF, and 216 HCF, respectively.
- vi. The energy losses through the side and bottom walls amounted to 30.45%, 26.15%, and 8.30%.

Acknowledgment

This research was funded by a grant from Universitas Sebelas Maret and the Ministry of Higher Education of Indonesia under the Fundamental Research contract number 1280.1/UN27.22/PT.01.03/2023. The article was presented during ICESEAM 2023, and sincere gratitude is extended to all the committee members who assessed and provided insightful suggestions to improve the content.

References

- [1] Kabeel, A. E., Mohamed Abdelgaied, K. Harby, and Amr Eisa. "Augmentation of diurnal and nocturnal distillate of modified tubular solar still having copper tubes filled with PCM in the basin." *Journal of Energy Storage* 32 (2020): 101992. <https://doi.org/10.1016/j.est.2020.101992>
- [2] Sharon, H. K. S. R., and K. S. Reddy. "A review of solar energy driven desalination technologies." *Renewable and Sustainable Energy Reviews* 41 (2015): 1080-1118. <https://doi.org/10.1016/j.rser.2014.09.002>
- [3] Mevada, Dinesh, Hitesh Panchal, Kishor Kumar Sadasivuni, Mohammad Israr, M. Suresh, Swapnil Dharaskar, and Hemin Thakkar. "Effect of fin configuration parameters on performance of solar still: a review." *Groundwater for Sustainable Development* 10 (2020): 100289. <https://doi.org/10.1016/j.gsd.2019.100289>
- [4] IRENA. "Water Desalination Using Renewable Energy - Technology Brief." *International Renewable Energy Agency*, 2012.
- [5] Al-Karaghoul, Ali A., and L. L. Kazmerski. "Renewable energy opportunities in water desalination." *Desalination, Trends and Technologies* (2011): 149-184.
- [6] Haddad, Zakaria, Abla Chaker, Azzedine Nahoui, Mohamed Salmi, and Islam Laifa. "Experimental Study of an Inclined Wick Solar Still Operating in Drop by Drop System Under The Climatic Conditions of Hodna's Region, Algeria." *Journal of Advanced Research in Fluid Mechanics and Thermal Sciences* 94, no. 1 (2022): 188-199. <https://doi.org/10.37934/arfmts.94.1.188199>
- [7] Septiyanto, Muhamad Dwi, Eko Prasetya Budiana, Ari Prasetyo, and Syamsul Hadi. "The Using of Thermal Energy Storage on Single Slope Solar Still Distiller." In *E3S Web of Conferences*, vol. 465, p. 01023. EDP Sciences, 2023. <https://doi.org/10.1051/e3sconf/202346501023>
- [8] Elsheikh, Ammar H., S. Shanmugan, Ravishankar Sathyamurthy, Amrit Kumar Thakur, Mohamed Issa, Hitesh Panchal, T. Muthuramalingam, Ravinder Kumar, and Mohsen Sharifpur. "Low-cost bilayered structure for improving the performance of solar stills: Performance/cost analysis and water yield prediction using machine learning." *Sustainable Energy Technologies and Assessments* 49 (2022): 101783. <https://doi.org/10.1016/j.seta.2021.101783>
- [9] Singh, Rupinder Pal, Haoxin Xu, S. C. Kaushik, Dibakar Rakshit, and Alessandro Romagnoli. "Effective utilization of natural convection via novel fin design & influence of enhanced viscosity due to carbon nano-particles in a solar cooling thermal storage system." *Solar Energy* 183 (2019): 105-119. <https://doi.org/10.1016/j.solener.2019.03.005>
- [10] Suraparaju, Subbarama Kousik, Arivazhagan Sampathkumar, and Sendhil Kumar Natarajan. "Experimental and economic analysis of energy storage-based single-slope solar still with hollow-finned absorber basin." *Heat Transfer* 50, no. 6 (2021): 5516-5537. <https://doi.org/10.1002/htj.22136>
- [11] Hafs, Hajar, Mohamed Asbik, Hassane Boushaba, Abdelghani Koukouch, Anass Zaaoumi, Abdellah Bah, and Omar Ansari. "Numerical simulation of the performance of passive and active solar still with corrugated absorber surface as heat storage medium for sustainable solar desalination technology." *Groundwater for Sustainable Development* 14 (2021): 100610. <https://doi.org/10.1016/j.gsd.2021.100610>
- [12] Jahanpanah, Maryam, Seyyed Javad Sadatinejad, Alibakhsh Kasaeian, Mohammad Hossein Jahangir, and Hamid Sarrafha. "Experimental investigation of the effects of low-temperature phase change material on single-slope solar still." *Desalination* 499 (2021): 114799. <https://doi.org/10.1016/j.desal.2020.114799>
- [13] Benhammou, M., and Y. Sahl. "Energetic and exergetic analysis of a sloped solar still integrated with a separated heat storage system incorporating phase change material." *Journal of Energy Storage* 40 (2021): 102705. <https://doi.org/10.1016/j.est.2021.102705>
- [14] Kumar, P. Manoj, Prashant Chauhan, Amit Kumar Sharma, Moti Lal Rinawa, A. J. Rahul, M. Srinivas, and A. Tamilarasan. "Performance study on solar still using nano disbanded phase change material (NDPCM)." *Materials Today: Proceedings* 62 (2022): 1894-1897. <https://doi.org/10.1016/j.matpr.2022.01.050>
- [15] Abdelaziz, Gamal B., Almoataz M. Algazzar, Emad MS El-Said, Ashraf Mimi Elsaid, Swellam W. Sharshir, A. E. Kabeel, and S. M. El-Behery. "Performance enhancement of tubular solar still using nano-enhanced energy storage material integrated with v-corrugated aluminum basin, wick, and nanofluid." *Journal of Energy Storage* 41 (2021): 102933. <https://doi.org/10.1016/j.est.2021.102933>
- [16] Yousef, Mohamed S., Hamdy Hassan, S. Kodama, and H. Sekiguchi. "An experimental study on the performance of single slope solar still integrated with a PCM-based pin-finned heat sink." *Energy Procedia* 156 (2019): 100-104. <https://doi.org/10.1016/j.egypro.2018.11.102>
- [17] Kateshia, Jyotin, and Vikas J. Lakhera. "Analysis of solar still integrated with phase change material and pin fins as absorbing material." *Journal of Energy Storage* 35 (2021): 102292. <https://doi.org/10.1016/j.est.2021.102292>
- [18] El-Sebaili, A. A., M. R. I. Ramadan, S. Aboul-Enein, and M. El-Naggar. "Effect of fin configuration parameters on single basin solar still performance." *Desalination* 365 (2015): 15-24. <https://doi.org/10.1016/j.desal.2015.02.002>

- [19] Elgendi, Mahmoud, Abd Elnaby Kabeel, and Fadl Abdelmonem Essa. "Application of heat sinks inside the pyramid solar distiller: experimental study on distiller performance under various operating conditions." *Environmental Science and Pollution Research* 30, no. 8 (2023): 21838-21852. <https://doi.org/10.1007/s11356-022-23779-y>
- [20] Mirmanto, I. Made Adi Sayoga, Agung Tri Wijayanta, Agus Pulung Sasmito, and Muhammad Aziz. "Enhancement of continuous-feed low-cost solar distiller: effects of various fin designs." *Energies* 14, no. 16 (2021): 4844. <https://doi.org/10.3390/en14164844>
- [21] Fayaz, H., Sayfar Rasachak, Muhammad Shakeel Ahmad, Laveet Kumar, Bo Zhang, M. A. Mujtaba, Manzoore Elahi M. Soudagar, Ravinder Kumar, and Mohammad Rasoul Omidvar. "Improved surface temperature of absorber plate using metallic titanium particles for solar still application." *Sustainable Energy Technologies and Assessments* 52 (2022): 102092. <https://doi.org/10.1016/j.seta.2022.102092>
- [22] Abdelgaied, Mohamed, Yehya Zakaria, A. E. Kabeel, and Fadl A. Essa. "Improving the tubular solar still performance using square and circular hollow fins with phase change materials." *Journal of Energy Storage* 38 (2021): 102564. <https://doi.org/10.1016/j.est.2021.102564>
- [23] Wang, Wen-Qi, Yu Qiu, Ming-Jia Li, Feng Cao, and Zhan-Bin Liu. "Optical efficiency improvement of solar power tower by employing and optimizing novel fin-like receivers." *Energy Conversion and Management* 184 (2019): 219-234. <https://doi.org/10.1016/j.enconman.2018.12.029>
- [24] Jani, Hardik K., and Kalpesh V. Modi. "Experimental performance evaluation of single basin dual slope solar still with circular and square cross-sectional hollow fins." *Solar Energy* 179 (2019): 186-194. <https://doi.org/10.1016/j.solener.2018.12.054>
- [25] Alaian, W. M., E. A. Elnegiry, and Ahmed M. Hamed. "Experimental investigation on the performance of solar still augmented with pin-finned wick." *Desalination* 379 (2016): 10-15. <https://doi.org/10.1016/j.desal.2015.10.010>
- [26] Appadurai, M., and V. Velmurugan. "Performance analysis of fin type solar still integrated with fin type mini solar pond." *Sustainable Energy Technologies and Assessments* 9 (2015): 30-36. <https://doi.org/10.1016/j.seta.2014.11.001>
- [27] Velmurugan, V., M. Gopalakrishnan, R. Raghu, and K. Srithar. "Single basin solar still with fin for enhancing productivity." *Energy Conversion and Management* 49, no. 10 (2008): 2602-2608. <https://doi.org/10.1016/j.enconman.2008.05.010>
- [28] Rabhi, Kamel, Rached Nciri, Faouzi Nasri, Chaouki Ali, and Habib Ben Bacha. "Experimental performance analysis of a modified single-basin single-slope solar still with pin fins absorber and condenser." *Desalination* 416 (2017): 86-93. <https://doi.org/10.1016/j.desal.2017.04.023>
- [29] Manokar, A. Muthu, and D. Prince Winston. "Experimental analysis of single basin single slope finned acrylic solar still." *Materials Today: Proceedings* 4, no. 8 (2017): 7234-7239. <https://doi.org/10.1016/j.matpr.2017.07.051>
- [30] Rajaseenivasan, T., and K. Srithar. "Performance investigation on solar still with circular and square fins in basin with CO₂ mitigation and economic analysis." *Desalination* 380 (2016): 66-74. <https://doi.org/10.1016/j.desal.2015.11.025>
- [31] Sharshir, S. W., A. H. Elsheikh, Guilong Peng, Nuo Yang, M. O. A. El-Samadony, and A. E. Kabeel. "Thermal performance and exergy analysis of solar stills-A review." *Renewable and Sustainable Energy Reviews* 73 (2017): 521-544. <https://doi.org/10.1016/j.rser.2017.01.156>
- [32] Nilsson, Thomas, and Roger Rowell. "Historical wood-structure and properties." *Journal of Cultural Heritage* 13, no. 3 (2012): S5-S9. <https://doi.org/10.1016/j.culher.2012.03.016>
- [33] Nagaraju, V., G. Murali, Anand K. Bewoor, Ravinder Kumar, Mohsen Sharifpur, Mamdouh El Haj Assad, and Mohamed M. Awad. "Experimental study on performance of single slope solar still integrated with sand troughs." *Sustainable Energy Technologies and Assessments* 50 (2022): 101884. <https://doi.org/10.1016/j.seta.2021.101884>
- [34] El-Sebaili, A. A. "Effect of wind speed on active and passive solar stills." *Energy Conversion and Management* 45, no. 7-8 (2004): 1187-1204. <https://doi.org/10.1016/j.enconman.2003.09.036>
- [35] Wirangga, Ristanto, Dan Mugisidi, Adi Tegar Sayuti, and Oktarina Heriyani. "The Impact of Wind Speed on the Rate of Water Evaporation in a Desalination Chamber." *Journal of Advanced Research in Fluid Mechanics and Thermal Sciences* 106, no. 1 (2023): 39-50. <https://doi.org/10.37934/arfmts.106.1.3950>
- [36] Prakash, V., and V. Velmurugan. "Effect of Wind Speed and Water Depth on the Performance of a Solar Still." *Journal of Chemical and Pharmaceutical Sciences* (2015): 12-14.
- [37] Sachan, Vivek, and Ajeet Kumar Rai. "Studies on finned basin solar still." *International Journal of Mechanical Engineering and Technology* 7, no. 3 (2016): 119-124.
- [38] Wang, Wen-Qi, Yu Qiu, Ming-Jia Li, Feng Cao, and Zhan-Bin Liu. "Optical efficiency improvement of solar power tower by employing and optimizing novel fin-like receivers." *Energy Conversion and Management* 184 (2019): 219-234. <https://doi.org/10.1016/j.enconman.2018.12.029>

- [39] Panchal, Hitesh, Rajan Petkar, Chandrakant Sonawane, Kishor Kumar Sadasivuni, Hagar Alm El Din Mohamad, and Pradeep Boka. "Use of computational fluid dynamics for solar desalination system: a review." *International Journal of Ambient Energy* 43, no. 1 (2022): 5742-5757. <https://doi.org/10.1080/01430750.2021.1965019>
- [40] Psiloglou, B. E., M. Santamouris, and D. N. Asimakopoulos. "On the atmospheric water vapor transmission function for solar radiation models." *Solar Energy* 53, no. 5 (1994): 445-453. [https://doi.org/10.1016/0038-092X\(94\)90059-0](https://doi.org/10.1016/0038-092X(94)90059-0)
- [41] Montgomery, Douglas C. "Chapter 4 - Randomized Block, Latin Square, and Related Designs Solutions." *Design and Analysis of Experiments* (2001): 126-169.